Investigation of spectroscopic properties and energy transfer between Ce and Dy in (Lu0.2Gd0.8−x−yCexDyy)2SiO5 single crystals

ARTICLE *in* JOURNAL OF LUMINESCENCE · MAY 2015

Impact Factor: 2.72 · DOI: 10.1016/j.jlumin.2015.05.013

6 AUTHORS, INCLUDING:

I. R. Martin
Universidad de La Laguna
231 PUBLICATIONS **2,092** CITATIONS
SEE PROFILE

Michal Glowacki
Institute of Physics of the Polish Academy o…
15 PUBLICATIONS **60** CITATIONS
SEE PROFILE

Witold Ryba-Romanowski
Polish Academy of Sciences
322 PUBLICATIONS **3,141** CITATIONS
SEE PROFILE

Carla Perez-Rodriguez
Universidad de La Laguna
20 PUBLICATIONS **134** CITATIONS
SEE PROFILE

Journal of Luminescence 166 (2015) 304–312

Contents lists available at ScienceDirect

Journal of Luminescence

journal homepage: www.elsevier.com/locate/jlumin

Investigation of spectroscopic properties and energy transfer between Ce and Dy in $(Lu_{0.2}Gd_{0.8-x-y}Ce_xDy_y)_2SiO_5$ single crystals

A. Strzęp [a,*], I.R. Martin [b,c], M. Głowacki [d], W. Ryba-Romanowski [a], M. Berkowski [d], C. Pérez-Rodríguez [b,c]

[a] Institute of Low Temperature and Structure Research PAS, Wroclaw, Poland
[b] Faculty of Physics, Universidad de La Laguna, S/C de Tenerife, Spain
[c] Malta Consolider Team and Instituto de Materiales y Nanotecnología (IMN), Universidad de La Laguna, S/C de Tenerife, Spain
[d] Institute of Physics PAS, Warsaw, Poland

ARTICLE INFO

Article history:
Received 17 November 2014
Received in revised form
27 April 2015
Accepted 10 May 2015
Available online 29 May 2015

Keywords:
Luminescence and amplification measurements
Single crystal
Energy transfer

ABSTRACT

In this paper we present results of spectroscopic investigations of single crystals with general formula $(Lu_{0.2}Gd_{0.8-x-y})_2SiO_5$ codoped with x% of Ce^{3+} and y% of Dy^{3+} ions. Investigated materials exhibit strong optical anisotropy what can be easily observed in polarized absorption and emission spectra. Based on room temperature polarized absorption spectra calculations in framework of phenomenological Judd–Ofelt model was carried out. Intensity parameters Ω_t were evaluated to be $\Omega_2=7.08$ (± 0.39), $\Omega_4=2.76$ (± 0.44), and $\Omega_6=3.36$ (± 0.21) [10^{-20} cm^2] for sample doped with 1% of cerium and $\Omega_2=10.72$ (± 0.33), $\Omega_4=1.98$ (± 0.37), and $\Omega_6=2.11$ (± 0.18) [10^{-20} cm^2] for sample doped with 3% of cerium. Influence of cerium admixture on Judd Ofelt intensity parameters is discussed. Value of experimental lifetime of $_4F_{9/2}$ multiplet of Dy^{3+} ion in sample doped with 1 at% Ce is 0.5 ms ($\tau_{rad}=0.45$ ms), while for sample doped with 3 at% of Ce, experimental lifetime is 0.45 ms ($\tau_{rad}=0.43$ ms). Absorption bands located between 440 and 460 nm, can be utilized for optical pumping of material by GaN laser diodes. Intense and broad emission bands at 465–495 and 560–590 nm, with experimental branching ratio strongly depending on polarization, give high chance for obtaining white luminophore, due to appropiate mixing of blue and yellow luminescence. By means of a pump and probe experiment optical amplification was demonstrated in the codoped sample with 1 at% of Ce and 1 at% Dy at 575 nm corresponding to the emission of Dy^{3+} with a high net gain coefficient of 34 cm^{-1}. Such high amplification was obtained under 359 nm excitation (at the maximum of intense absorption band of Ce^{3+} ions).

1. Introduction

Oxyorthosilicates with general formula RE_2SiO_5 form a group of known but still intensively studied materials. Lu_2SiO_5 or Gd_2SiO_5 crystals doped with cerium, usually denoted as LSO:Ce or GSO:Ce respectively, belong to most common scintillation materials [1]. RE_2SiO_5 doped with lanthanide ions such as Nd^{3+}, Sm^{3+}, Eu^{3+}, Tb^{3+}, Dy^{3+}, Er^{3+},and Yb^{3+} can find potential application as phosphors [2] or laser materials [3]. Crystal structure of RE_2SiO_5 (RE=Sc^{3+}, Y^{3+}, Gd^{3+},and Lu^{3+}) belongs to monoclinic system. Usually aforementioned oxyorthosilicates crystallize in C2/c space group. Exception is Gd_2SiO_5 which crystallizes in $P2_1/c$ space group. LSO and GSO systems exhibit continuous solubility in solid state; however, due to different space groups of pure components, phase change must be forced for exact value of lutetium concentration. For $(Lu_xGd_{1-x})_2SiO_5$ solid state solution this phase change occurs when x is less than 0.17 [4]. A great disadvantage of solution crystallized in $P2_1/c$ space group, contrary to C2/c, is the tendency to crack along cleavage plane, what leads to problems during mechanical processing of this material. A very high melting temperature ($T_m=2060$ °C) which is close to thermal breakdown of iridium crucible and heat insulation of stabilized zirconia ceramics is a disadvantage of pure Lu_2SiO_5 crystals. Introduction of solid state solution of GSO and LSO gives two advantages. Firstly melt temperature of solution can be reduced by ca. 200 K in comparison to melt temperature of pure LSO [4]. Secondly huge amount of expensive Lu_2O_3 can be substituted by relatively cheaper Gd_2O_3. Sidletskiy et al. [5] discuss other practical aspects of substitution of Lu ions by the Gd ones. They suggested that such substitution will efficiently reduce the difference between ionic radius of Lu^{3+} and lanthanide ions from beginning of lanthanide series such as Ce^{3+} or Pr^{3+}, which will lead to smaller

* Corresponding author.

http://dx.doi.org/10.1016/j.jlumin.2015.05.013
0022-2313/

concentration gradient and more homogenous distribution of dopant along pulled crystal boule.

Trivalent dysprosium ion exhibits two strong emission bands that can be related to transitions from $^4F_{9/2}$ to ^6H_J ($J=15/2, 13/2$) multiplets. First one of them occurs at blue part of spectrum, while second one in yellow part. Transition in yellow part of spectrum belongs to hypersensitive transitions, (intensity is strongly affected by crystal environment), so even a small change in distance to surrounding ions could lead to big change of luminescence intensity dissipation between $^4F_{9/2}$–$^6H_{15/2}$ and $^4F_{9/2}$–$^6H_{13/2}$ transitions. From CIE 1931 chromatic diagram it emerged that white light could be obtained by appropriate mixture of blue and yellow lights. A suitable yellow/blue ratio varying with host composition can control the luminescence color of materials doped with Dy^{3+} ions.

This work is aimed at an assessment of spectroscopic properties of dysprosium and cerium codoped $(Lu_{0.2}Gd_{0.8-x-y})_2SiO_5$ single crystals. Motivation of incorporation of cerium was to enhance luminescence related to $^4F_{9/2}$–^6H_J ($J=15/2, 13/2$) transition of Dy^{3+} ion, by energy transfer from Ce to Dy. Trivalent dysprosium exhibits many broad but weak absorption bands above 480 nm, thus optical pumping of this lanthanide is nontrivial. Incorporation of Ce^{3+} ions that possess enormous intense absorption band is related to 4f–5d allowed transition centered at 350 nm (in GSO), which could increase luminescent response of Dy^{3+} ions if energy transfer between Ce and Dy occurs. For experiments $(Lu_{0.2}Gd_{0.78}Ce_{0.01}Dy_{0.01})_2SiO_5$ and $(Lu_{0.2}Gd_{0.76}Ce_{0.03}Dy_{0.01})_2SiO_5$ single crystals were grown by Czochralski technique.

Besides, the intense yellow emission of Dy^{3+} features potential for laser operation in the four-level-scheme as is reported in Ref. [6] where the gain dynamics of this process has also been analyzed. For this reason pump and probe measurements have been performed in order to research the capabilities for optical amplification of the reported crystals. However, in our experiments the excitation has been carried out in the intense absorption band of the Ce^{3+} ions in order to obtain an efficient transfer to Dy^{3+} ions and a high value for the gain amplification.

2. Experimental

Single crystal of $(Lu_{0.2}Gd_{0.8})_2SiO_5$ codoped with Dy^{3+} and Ce^{3+} ions (1:1 and 1:3 at%) was grown by the Czochralski method. Purity grade of starting materials was as follows: Gd_2O_3 (4N), Lu_2O_3 (4N), SiO_2 (5N), Dy_2O_3 (5N), and CeO_2 (4N5). Crystals were pulled on iridium rod. Crystals were oriented exploiting Laue method, and cut into slices perpendicular to ⟨0 1 0⟩ plane.

All orthorhombic, monoclinic and triclinic crystals are optically biaxial. In monoclinic system one of the optical indicatrix is collinear with crystallographic *b* axis. Cross polarized polarizing microscope was used to determine directions in which crystal slice does not pass light (directions of two other indicatrix have been revealed). A sample in the form of a $6\times6\times6$ mm^3 cube was cut along determined directions out of the crystal slice and polished for measurement. Conoscopic figures were observed from obtained samples with use of confocal polarizing microscope. Bisectrix figures were observed for the sample which normal to the plane was collinear to crystallographic *b* axis. Due to lack of sufficient equipment we were unable to determine exact values of n_α, n_β, and n_γ, so we cannot assign if crystal is optically positive or negative, nor can we estimate value of inclination angle of optical axes.

Absorption spectra were recorded with a Varian 5E UV–vis–NIR spectrophotometer. Instrument spectral bandwidth was set to 0.25 nm in UV–vis (300–800 nm) and 1 nm in IR (800–2500 nm) region. Emission spectra were recorded using Dongwoo Optron System containing a DM 158i excitation monochromator and a DM711 emission monochromator. The 150 W ozone free Xenon lamp DL 80-Xe and Ar^+ CW laser were used as excitation sources. Luminescence decay curves were measured with Tektronix Model TDS 3052 digital oscilloscope. Continuum Surelite I Optical Parametric Oscillator pumped by a third harmonic of Nd:YAG laser was used as an excitation source. For low temperature measurement a continuous-flow liquid helium cryostat (OXFORD INSTRUMENTS model CF 1204) equipped with a temperature controller was used. Polarized spectra were measured exploiting Harrick PGT-S1V Glan–Taylor polarizers. Measurements of optical amplification were carried out in a pump and probe experimental setup whose scheme can be found elsewhere [6]. The pump radiation was provided by an optical parametric oscillator (OPO) syntonized at 359 nm with energy pulses between 0.25 and 5.7 mJ/cm^2 of about 5 ns of duration. The probe beam was obtained by a continuous 400 W lamp combined with a monochromator, resulting in a signal power density of 210 μW/cm^2 at 575 nm with a spectral width of 5 nm. The incidence of pump and probe beams (linearly polarized) were directed normal to the surface of the sample aligned to the crystallographic *b*-axis which was situated after a 1 mm diameter pinhole. A prism was employed to align both the beams. In order to cover only the whole area of the pinhole, the pump beam was focused by a 20 cm focal length lens. The detection chain was formed by a TRIAX-180 monochromator with 1 nm resolution and the output of the photomultiplier tube was registered by a digital oscilloscope TEKTRONIX-2430 A for temporal analysis of the decay curves. To determine the optical gain, two kinds of emission spectra were measured. In the first one, the pump and probe beams were present simultaneously, while in the second one the probe was blocked.

3. Crystallographic and optical characterization

Investigated crystals belong to monoclinic crystal system, with space group C2/c for sample doped with 1 at% of Ce and $P2_1/c$ for sample doped with 3 at% of Ce (both samples are also doped with 1 at% of Dy). According to the work of Glowacki [4], when the "*x*" is less than 0.84 undoped $(Lu_{1-x}Gd_x)_2SiO_5$ crystals tend to grow in $P2_1/c$ space group (GSO structure). In investigated samples *x* is equal to 0.78 and 0.76 for samples doped with 1 at% Dy and 1 at% or 3 at% of Ce respectively. Sample with $x=0.78$ follows the rule shown in the work of Glowacki et al.; however, admixture of 3 at% of cerium forced phase change from C2/c to $P2_1/c$ space group. This could be explained by the fact, that medium size Gd^{3+} ions are replaced by much bigger Ce^{3+} ions. Phase transition between GSO and LSO structures occurs at appropriate big/small cations ratio.

In crystal structures of Lu_2SiO_5 and Gd_2SiO_5, which are isostructural with samples doped with 1 at% of Ce and with 3 at% of Ce respectively, two different crystallographic sites occur, which are characterized in Table 1. Information about ionic radii of elements occurring in samples investigated is gathered in Table 2.

3.1. Case of Lu_2SiO_5 type structure

Taking into consideration standard deviation of Ln–O distance in both sites, one can assume, that Ln–O distances in Ln2 are quite uniform, while Ln–O distances in Ln1 are more heterogeneous. Non-uniform distribution of oxygen ions in Ln1 should result in better adaptation of oxygen ligands for ions with bigger ionic radius. Comparison of available $r_{(Ln)}$ with ionic radii of ions incorporated into crystal leads to the conclusion that Ln2 site should be preferentially occupied by Lu^{3+} and Ce^{4+}. However

Table 1
Crystallograpic characteristic of two Ln^{3+} sites in Lu_2SiO_5 and Gd_2SiO_5 taken from[a] [15,16].

Lu_2SiO_5	Ln1	Ln2
Coordination number (CN)	7	6
Local symmetry	C_1	C_1
Ln–O mean [Å]	2.325	2.228
Ln–O min [Å]	2.160	2.166
Ln–O max [Å]	2.616	2.262
Ln–O standard deviation (σ) [Å]	**0.142**	**0.032**
Ln_X–Ln_X min distance [Å]	3.587	3.425
Ln1–Ln2 min distance [Å]	3.345	
Available $r_{(LnX)}$[a] [Å]	**0.925**	**0.828**
Gd_2SiO_5	Ln1	Ln2
Coordination number (CN)	9	7
Local symmetry	C_1	C_1
Ln–O mean [Å]	2.487	2.387
Ln–O min [Å]	2.273	2.295
Ln–O max [Å]	2.761	2.532
Ln–O standard deviation (σ) [Å]	**0.164**	**0.098**
Ln_X–Ln_X min distance [Å]	3.362	3.519
Ln1–Ln2 min distance [Å]	3.728	
Available $r_{(LnX)}$[a] [Å]	**1.087**	**0.987**

[a] Available r(Ln) was calculated by subtraction of 1.40 (value of ionic radius of O^{2-}) from value of mean Ln–O distance.

Table 2
Value of mean ionic radius (Ir) of elements occupying crystallograpic sites with different coordination numbers in oxide crystals [17].

	Ir (CN=VI) [Å]	Ir[a] (CN=VII) [Å]	Ir (CN=VIII) [Å]	Ir[b] (CN=IX) [Å]
O^{2-}	1.40	1.41	1.42	1.43
Ce^{3+}	1.034	1.087	1.14	1.193
Gd^{3+}	0.938	0.999	1.06	1.121
Dy^{3+}	0.908	0.969	1.03	1.091
Lu^{3+}	0.848	0.909	0.97	1.031
Ce^{4+}	0.80	0.885	0.97	1.055
Si^{4+}	0.26 (CN=IV)			

[a] Calculated as mean value between Ir^{VI} and Ir^{VIII}.
[b] Calculated as $Ir^{VIII}+\Delta(Ir^{VIII}-Ir^{VII})$.

incorporation of Ce^{4+} in site of Ln^{3+} will lead to charge mismatch, which could result in the formation of point defects such as colour centers. Available $r_{(Ln1)}$ is a little bit higher than Ir^{VII} of Ce^{4+} and Lu^{3+}, and a little bit lower than Ir^{VII} of Dy^{3+} and Gd^{3+}. Ionic radius (CN=VII) of Ce^{3+} is 0.162 Å higher than $r_{(Ln1)}$, so incorporation of this ion into this site will lead to relatively high expansion of coordination polihedra and shrinkage of adjacent coordination polihedras. This change of position of ions modifies local crystal field which can, slightly but noticeably, affect energy of $^{2S+1}L_J(\alpha)$ Stark levels of lanthanide ions incorporated into matrix. In a similar way, but on smaller scale, other lanthanide ions present in crystal act. Above-mentioned energy differences lead to the broadening of absorption and emission bands, what in an extreme case, can change shape of bands from "crystalline" to "glassy" type (such a behavior can be clearly noticed, when we compare absorption spectra of dysprosiom doped $(Lu_xGd_{1-x})_2SiO_5$ crystals shown in the work of Dominiak-Dzik [7]. Arguments described above lead to a conclusion that in investigated material two groups of crystalline environment occur instead of two strictly defined sites.

3.2. Case of Gd_2SiO_5 type structure

Both crystallographic sites of Ln^{3+} ions in GSO structure possess higher $r_{(LnX)}$ contrary to LSO structure. Comparing $r_{(LnX)}$ with estimated ionic radii gathered in Table 2, one can conclude that Ln1 site should be preferentially occupied by Dy^{3+}, Gd^{3+} or Ce^{4+} ions. Occupation of this site by little bit smaller Lu^{3+} will lead to shrinkage of Ln1 coordination polihedra, and expansion of adjacent one, while occupation of this site by Ce^{3+} will act in reverse way. However, when taking into account, relatively high, standard deviation of Ln–O distances for this site, one cannot exclude possibility of occupation of this site by every chemical species present in matrix. Ln2 site, which is coordinated by 7 oxygens possesses more uniform distribution of Ln–O distances, so expansion or contraction should be more tough. This site is well suited for Gd^{3+}, Dy^{3+} and is moderate for Lu^{3+}. Ionic radius of Ce^{3+} and Ce^{4+} is 0.1 Å bigger or smaller, than $r_{(LnX)}$ of this site respectively, so occupation factor of cerium ions in this site should be rather low. Similar discussion on possibility of occupation by Dy^{3+} ion both Gd^{3+} sites in GSO matrix was conducted in [7a].

3.3. Optical anisotropy

In monoclinic crystals one of the optical indicatrices is collinear with crystallographic b axis, which is the principal axis in monoclinic systems ($\beta \neq 90°$). Direction of two other optical indicatrices was found by use of cross polarized microscope. Directions of those indicatrices will be denoted in this work as X and Y. Measurements were performed on samples whose edges were cut parallel to optical indicatrices of the crystal. Three different polarized spectra were recorded due to optical anisotropy of investigated crystal.

4. Absorption characteristics, linewidths and thermal shifts of lines

Polarized absorption spectra for samples both doped with 1 at% of Dy^{3+} and codoped with 1 at% of Ce^{3+} or 3 at% of Ce^{3+} are shown in Figs. 1 and 2 respectively. They reveals strong optical anisotropy of investigated materials. Higher concentration of cerium forced change in space group where the crystal prefers to grow. The same effect was observed in LGSO solid state solution singly doped with Ce, where $(Lu_{0.2}Gd_{0.8-x})_2SiO_5$ crystal doped with $x=0.006$ Ce grows in GSO structure type, while crystal with $x=0.0045$ grows in LSO structure type [5]. From our growth experiments it emerges that the admixture of 1 at% of Dy^{3+}, that

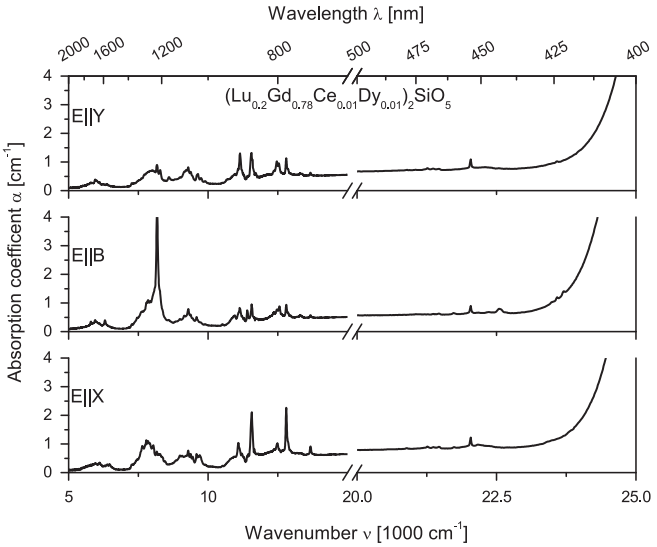

Fig. 1. Survey polarized absorption spectra of sample doped with 1 at% of Ce and 1 at% of Dy recorded at room temperature.

possesses little bit smaller ionic radius than Gd^{3+}, moves phase shift region induced by the presence of Ce^{3+}, which possesses higher ionic radius than Gd^{3+} to x values between 0.03 and 0.01.

In both the samples absorption spectra are dominated by lines located in near infrared, related to spin allowed transitions between ground state multiplet $^6H_{15/2}$ and multiplets ^6H_J (J=11/2, 9/2, 7/2, and 5/2) and ^6F_J (J=11/2, 9/2, 7/2, 5/2, 3/2, and 1/2). In this group both the transitions $^6H_{15/2}\rightarrow{}^6H_{11/2}$ and $^6H_{15/2}\rightarrow{}^6F_{11/2}$ can be considered as hypersensitive ones ($\Delta J=\pm 2$). Comparing squared reduced matrix elements $\|U^t\|^2$ (t=2, 4, and 6) [8] for transitions that can be related to bands located ca. 5880 cm^{-1} and 7800 cm^{-1} (listed in Table 3) and taking into account obtained Ω_t (t=2, 4, 6) Judd–Ofelt intensity parameters, it is easy to conclude that transition ca. 7800 cm^{-1} will be dominating in IR part of absorption spectra of both samples.

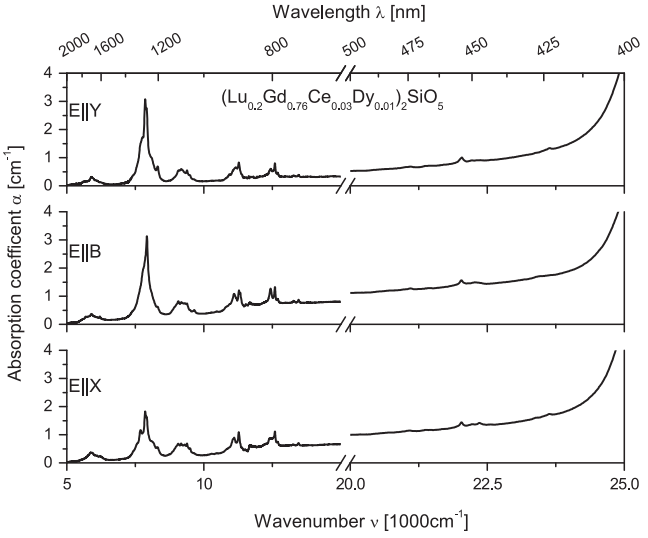

Fig. 2. Survey polarized absorption spectra of sample doped with 3 at% of Ce and 1 at% of Dy recorded at room temperature.

Table 3
Value of reduced matrix elements $\|U^t\|^2$ (t=2, 4, 6) [8] of some transitions within electronic structure of Dy^{3+} ion and obtained Judd–Ofelt intensity parameters Ω [$\times 10^{-20}$ cm^2] calculated for samples investigated.

$^6H_{15/2}\rightarrow$	Energy [cm^{-1}]	$\|U^2\|^2$	$\|U^4\|^2$	$\|U^6\|^2$
$^6H_{11/2}$	5880	0.0960	0.0340	0.6147
$^6H_{9/2}$	7800	0.9349	0.8310	0.2002
$^6F_{11/2}$	7800	0	0.0177	0.1985
$^4F(3)_{9/2}$	21,150	0	0.0049	0.0303
$^4I(3)_{15/2}$	22,100	0.0072	0.0003	0.0648
$^4G(4)_{11/2}$	23,400	0.0004	0.0146	0.0003
$^6P_{5/2}$	28,040	0	0	0.0720
$^6P_{7/2}$	28,650	0	0.5243	0.0127

	Ω_2	Ω_4	Ω_6
1 at% of Ce^{3+}	7.08 ($\pm$0.39)	2.76 ($\pm$0.44)	3.36 ($\pm$0.21)
3 at% of Ce^{3+}	10.72 ($\pm$0.33)	1.98 ($\pm$0.37)	2.11 ($\pm$0.18)

In visible part of spectrum, between 500 and 400 nm, three bands occur, that can be assigned to spin forbidden transitions from ground state to multiplets $^4F(3)_{9/2}$, $^4I(3)_{15/2}$ and $^4G(4)_{11/2}$. Their experimental intensity is scant, what is in good agreement with their $\|U^t\|^2$ parameters. The sextet term, ^6P to which spin allowed transitions are possible and which possesses energy > 20,000 cm^{-1}, is unable to observe due to absorption bands related to the presence of cerium ions. The presence of cerium affects absorption spectra in two following ways:

1. Cerium ions embedded in Gd_2SiO_5 and Lu_2SiO_5 crystals which exhibit strong absorption band related to parity allowed 5d $^\circ 4f^1$–$5d^14f^\circ$ transition, that spreads above $\lambda<420$ nm and $\lambda<380$ nm respectively [9].
2. Cerium ions in different compounds can have two oxidation states +3 or +4. Comparing the values of ionic radius of cerium ions in these two states one can notice that value of ionic radius of Ce^{4+} is very similar to value of ionic radius of Lu^{3+}. For a better match to crystallographic sites accessible in investigated compounds cerium can adopt +4 oxidation state. However due to charge mismatch between Ce^{4+} in Ln^{3+} site creation of point defects is expected. Those defects could possess their own absorption bands (therefore are named as "colour centers").

Polarized low temperature absorption spectra are shown in Figs. 3 and 4. Based on low temperature absorption spectra values of Stark levels energy of selected multiplets have been collected. This information is gathered in Tables 4 and 5.

From energy levels structure of Dy^{3+} scheme, that can be found elsewhere [10] emerge, that dysprosium ion embedded into oxide material possess one metastable level ($^4F(3)_{9/2}$). Absorption bands related to transitions from $^6H_{15/2}$ ground state multiplet to metastable $^4F(3)_{9/2}$, and two other closely spaced $^4I(3)_{15/2}$ and $^4G(4)_{11/2}$ levels can be observed in visible part of spectrum at ca. 21,300, 22,300 and 22,500 cm^{-1} respectively. For these three transitions the most intense line, that occurs in both the crystals at 22,038 cm^{-1} (453.75 nm) belongs to $^6H_{15/2}\rightarrow{}^4I(3)_{15/2}$ transition. This line could be used to optically pump material, with the use of appropriate InGaN/GaN laser diodes, thus influence of temperature on position, intensity and broadness of this line is a subject of

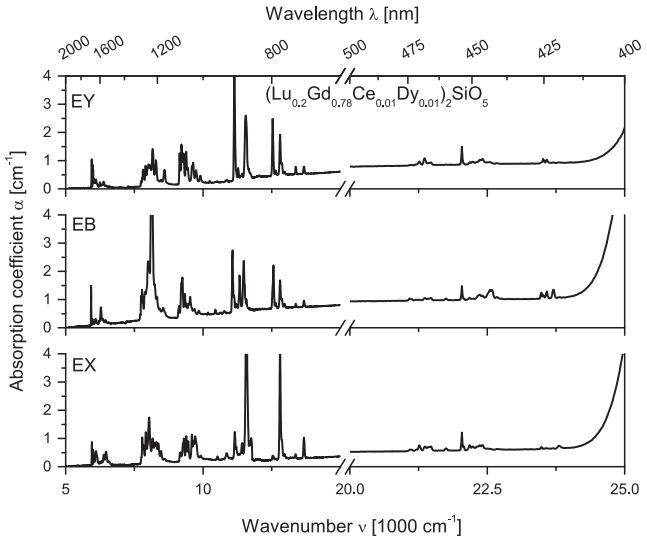

Fig. 3. Survey polarized absorption spectra of sample doped with 1 at% of Ce and 1 at% of Dy recorded at 5 K.

detailed analysis. Shape of line was fitted by pseudo-Voigt profiles and results are gathered in Fig. 5. Enormous broadness of absorption bands emerges from disordered nature of crystal sites in the materials investigated. However broad absorption lines are favorable for optical pumping of a luminescent material, especially when laser diodes are used for this purpose. Evaluated spectral bandwidth close to 100 cm^{-1} for 454 nm absorption line is comparable to spectral bandwidth of the high power multimode GaN/InGaN blue diode emission implying that high absorption efficiency can be achieved.

5. Judd–Ofelt analysis

Transition intensities of Dy^{3+} ions in the $(Lu_{0.2}Gd_{0.8-x-y})_2SiO_5$ crystal were analyzed in the framework of the Judd–Ofelt phenomenological model [11,12]. Polarized absorption spectra recorded at room temperature were used to calculate the oscillator strengths P_x, P_b and P_y. The intensities of absorption bands were evaluated by means of numerical employing Eq. (1)

$$P_A = \frac{mc}{\pi e^2 N}\int \alpha_A(\nu)d\nu \quad (1)$$

where A denotes the status of the light propagation direction, N means the density of dopant ions, m, e and c are the electron mass, electron charge and the velocity of light, respectively. $\alpha(\upsilon)$ is the absorption coefficient. This relation was applied to six bands located in the 5000–14,000 cm^{-1} spectral range and the procedure was repeated for each polarization state. For three bands oscillator strength was calculated holistically for a group of transitions from ground state to several closely spaced multiplets. This operation was made in order to reduce experimental uncertainties. Mean oscillator strength was calculated according to the following formula: $P_{mean}=(P_x+P_b+P_y)/3$. Obtained values of mean oscillator strengths were next used as input data for calculation in the framework of phenomenological Judd–Ofelt method. Obtained Ω_t ($t=$ 2, 4, 6) parameters are gathered in Table 6. These parameters were used to determine emission characteristic of the system under study. The radiative transition rates, luminescence branching ratios, and radiative lifetimes of excited state were estimated based on the Judd–Ofelt model. Obtained results are collected in Table 7.

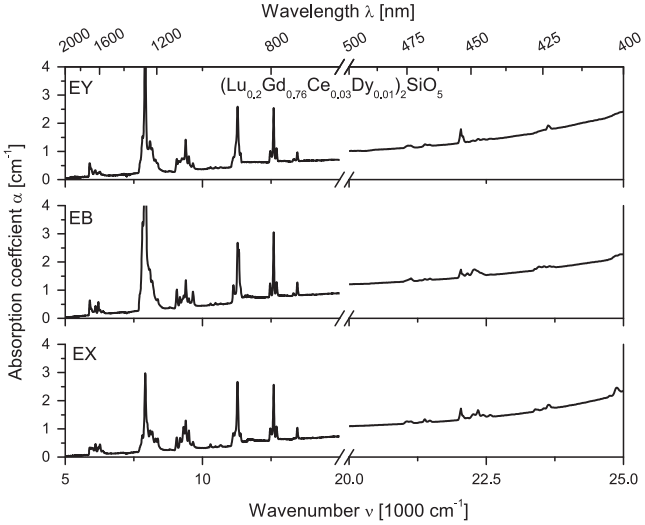

Fig. 4. Survey polarized absorption spectra of sample doped with 3 at% of Ce and 1 at% of Dy recorded at 5 K.

6. Luminescence characteristics

For each crystal investigated, at least three different luminescent centers occur. Two are represented by broad and fast decaying bands, while third has sharp and long lasting bands. Two fast decaying bands, can be attributed to 5d–4f transition within electronic structure of Ce^{3+} ions located in different crystallographic environments. Third luminescent center is related to dysprosium ions. Excitation and emission spectra recorded in 5 K and 300 K for both samples are shown in Fig. 6.

Broad band spreading in emission in ranges 400–550 and 425–600 nm (in Fig. 6(1–4) marked by black and red lines respectively) is related to Ce^{3+} ions embedded in the matrix. This statement is consistent with luminescence measurements of GSO:Ce crystal [13]. However for LSO structure type crystal emission from Ce^{3+} ions should possess maximum at ca. 400 nm [14], while strongest luminescence in investigated sample occurs at 440 nm (under 360 nm excitation) or at ca. 480 nm (under 395 nm excitation) at

Table 5
Values of energies, barycenters, energy splitting and number of experimentally observed Stark levels of selected multiplets in crystal doped with 1 at% of Dy and 3 at% of Ce.

$^6H_{15/2}\rightarrow$	Energy [cm^{-1}]	Barycenter	ΔE	N_{exp}	N_{theor}
$^6H_{11/2}$	5896, 5951, 6002, 6101, 6208, 6265, 6369	6113	473	7	2×6
$^6H_{9/2}$, $^6F_{11/2}$	7726, 7816, 7917, 8086, 8165, 8288, 8370	8053	644	7	$2\times5+2\times6$
$^6H_{7/2}$, $^6F_{9/2}$	9066, 9178, 9263, 9319, 9392, 9505, 9658	9340	592	7	$2\times4+2\times5$
$^6H_{5/2}$, $^6F_{7/2}$	11,132, 11,282, 11,325, 11,389	11,282	257	4	$2\times3+2\times4$
$^6F_{5/2}$	12,472, 12,597, 12,699	12,589	227	3	2×3
$^6F_{3/2,\ 1/2}$	13,323, 13,461	13,392	138	2	$2\times2+2\times1$
$^4F(3)_{9/2}$	21,123, 21,378, 21,470	21,324	347	3	2×5
$^4I(3)_{15/2}$	22,038, 22,161, 22,277, 22,352, 22,434, 22,573	22,306	535	6	2×8
$^4G(4)_{11/2}$	23,391, 23,460, 23,557, 23,645	23,513	254	4	2×6

Table 4
Values of energies, barycenters, energy splitting and number of experimentally observed Stark levels of selected multiplets in crystal doped with 1 at% of Dy and 1 at% of Ce.

$^6H_{15/2}\rightarrow$	Energy [cm^{-1}]	Barycenter	ΔE	N_{exp}	N_{theor}
$^6H_{11/2}$	5948, 5996, 6040, 6102, 6253, 6308, 6382, 6468, 6568	6229	620	9	2×6
$^6H_{9/2}$, $^6F_{11/2}$	7747, 7808, 7824, 7913, 7990, 8032, 8078, 8167, 8282, 8361, 8432, 8594	8102	847	12	$2\times5+2\times6$
$^6H_{7/2}$, $^6F_{9/2}$	9152, 9179, 9216, 9276, 9299, 9389, 9448, 9523, 9575, 9606, 9650, 9732, 9905	9458	753	13	$2\times4+2\times5$
$^6H_{5/2}$, $^6F_{7/2}$	11,152, 11,198, 11,273, 11,419, 11,567, 11,673	11,380	521	6	$2\times3+2\times4$
$^6F_{5/2}$	12,541, 12,638, 12,804, 12,867, 12,966	12,763	425	5	2×3
$^6F_{3/2,\ 1/2}$	13,371, 13,670	13,521	299	2	$2\times2+2\times1$
$^4F(3)_{9/2}$	21,108, 21,197, 21,265, 21,360, 21,425, 21,470, 21,750	21,368	642	7	2×5
$^4I(3)_{15/2}$	22,038, 22,185, 22,234, 22,360, 22,409, 22,548, 22,586, 22,675	22,379	637	8	2×8
$^4G(4)_{11/2}$	23,497, 23,580, 23,696, 23,809	23,646	312	4	2×6

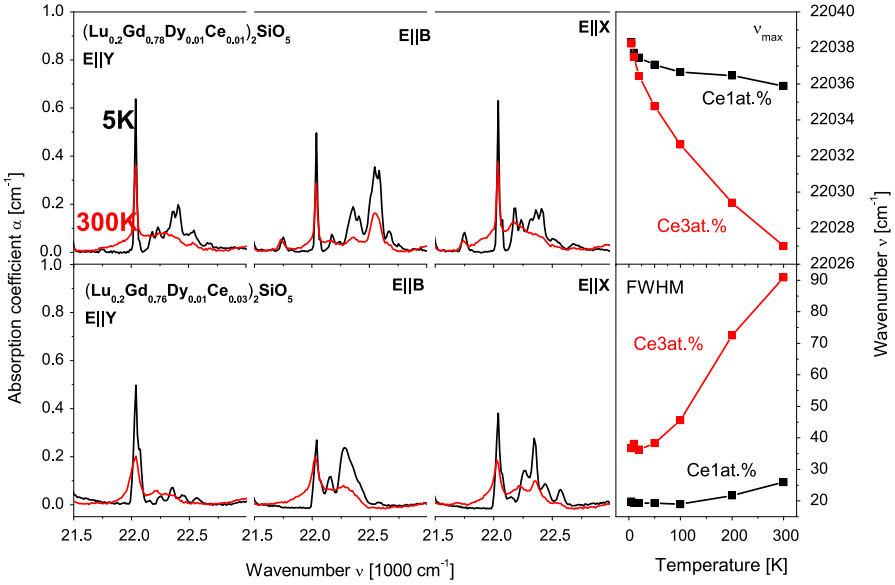

Fig. 5. Temperature and polarization influence on most prominent transition to multiplet lying above metastable $^4F_{9/2}$ level. Sample possessing LSO structure (1 at% Ce) exhibits scant influence of temperature and polarization on FWHM and υ_{max} of strongest line, contrary to sample possesing GSO structure.

Table 6
Experimental and calculated oscillator strengths for transitions elucidated from polarized room temperature absorption spectra of materials investigated.

Transition from $^6H_{15/2}$ to:		Energy [cm^{-1}]	Oscillator strength $\times 10^{-6}$					Residual $\Delta P \times 10^{-6}$
			P_x	P_b	P_y	Mean	Calc	
1 at% Dy 1 at% Ce	$^6H_{11/2}$	6003	1.82	2.13	2.39	2.12	2.26	0.14
	$^6F_{11/2}$, $^6H_{9/2}$,	8043	6.63	15.9	9.34	10.60	10.58	0.02
	$^6F_{9/2}$, $^6H_{7/2}$,	9291	4.81	4.27	5.53	4.87	4.91	0.04
	$^6F_{7/2}$, $^6H_{5/2}$,	11,428	4.33	3.15	5.06	4.18	4.07	0.11
	$^6F_{3/2}$	12,736	1.98	2.30	2.57	2.29	1.89	0.40
	$^6F_{1/2}$	13,566	0.08	0.08	0.31	0.16	0.36	0.20
	$\Omega_2=7.08$ ($\pm$0.39), $\Omega_4=2.76$ ($\pm$0.44), $\Omega_6=3.36$ ($\pm$ 0.21) [10^{-20} cm^2]							
1 at% Dy 3 at% Ce	$^6H_{11/2}$	5929	2.02	1.85	1.50	1.79	1.88	0.09
	$^6F_{11/2}$, $^6H_{9/2}$,	7846	9.54	14.08	15.13	12.92	12.88	0.04
	$^6F_{9/2}$, $^6H_{7/2}$,	9246	3.35	3.38	2.98	3.24	3.25	0.01
	$^6F_{7/2}$, $^6H_{5/2}$,	11,095	2.59	2.67	2.53	2.60	2.60	0.00
	$^6F_{3/2}$	12,525	1.68	1.88	1.22	1.59	1.19	0.30
	$^6F_{1/2}$	13,396	0.11	0.19	0.12	0.14	0.22	0.08
	$\Omega_2=10.72$ ($\pm$0.33), $\Omega_4=1.98$ ($\pm$0.37), $\Omega_6=2.11$ ($\pm$0.18) [10^{-20} cm^2]							

Table 7
Energies (υ), radiative transition rates for electric and magnetic dipole and branching ratios of $^4F(3)_{9/2} \rightarrow {}^6H_J$, ^6F_J transitions in investigated crystals. Data for MD was recalculated from [15].

	Multiplet	Wavenumber [cm^{-1}]	ED [s^{-1}]	MD[1] [s^{-1}]	β_{th} [%]	β_{exp} [%]
1 at% Dy 1 at% Ce	$^6H_{15/2}$	21,108	499.4	0	21.6	24.4
	$^6H_{13/2}$	17,009	1401.8	0	60.5	61.6
	$^6H_{11/2}$	15,237	147.8	17.6	7.1	5.8
	$^6H_{9/2}$	13,197	40.3	74.8	5.0	6.1
	$^6F_{11/2}$	12,939	37.3	4.0	1.8	
	$^6F_{9/2}$	11,892	4.6	8.2	0.6	2.1
	$^6H_{7/2}$	11,474	27.1	4.3	1.4	
	$^6H_{5/2}$	9960	12.3	0	0.5	
	$^6F_{7/2}$	9534	12.6	7.2	0.9	
	$^6F_{5/2}$	8345	17.0	0	0.7	
	$^6F_{3/2}$	7737	0.3	0	0.0	
	$^6F_{1/2}$	7438	0.2	0	0.0	
	Σ		2200.7	116.1	$\tau_{rad}=0.45$ ms	
1 at% Dy 3 at% Ce	$^6H_{15/2}$	21,123	318.8	0	13.1	38.1
	$^6H_{13/2}$	17,094	1637.6	0	67.2	50.2
	$^6H_{11/2}$	15,010	198.6	18.0	8.9	4.3
	$^6H_{9/2}$	13,033	42.9	76.9	4.9	5.4
	$^6F_{11/2}$	13,206	43.1	4.5	2.0	
	$^6F_{9/2}$	12,057	7.0	9.2	0.7	1.9
	$^6H_{7/2}$	11,725	24.5	4.9	1.2	
	$^6H_{5/2}$	10,000	8.5	0	0.3	
	$^6F_{7/2}$	9837	9.1	8.4	0.7	
	$^6F_{5/2}$	8534	24.8	0	1.0	
	$^6F_{3/2}$	7800	0.2	0	0.0	
	$^6F_{1/2}$	7662	0.2	0	0.0	
	Σ		2315.3	121.9	$\tau_{rad}=0.43$ ms	

room temperature. Decrease of temperature leads to redshift of maximum to ca. 520 nm. Described bands, are in fact composed of several overlapping lines, that are related to different luminescent centers. These centers are Ce^{3+} ions, but also luminescence forming point defects such as colour centers can be possible. In room temperature energy transfer between those luminescent centers occurs – which is confirmed by appropriate bands on excitation spectra. This transfer is moderate, thus we can observe dependence of maximum of luminescence on excitation wavelength. In lower temperatures energy transfer diminishes, thus influence of excitation wavelength on luminescent properties is much higher. This could be clearly seen when spectra of GSO structure type sample in 300 K and 5 K are compared. At room temperature maximum excitation spectra occur at ca. 395 nm. With decreasing temperature, excitation maximum of band peaking at 440 nm, blueshifts to 350 nm in 5 K.

Energy level structure of trivalent dysprosium ions reveals up to three potential metastable levels $^4F(3)_{9/2}$, $^4I(3)_{15/2}$ and $^4G(4)_{11/2}$. In oxide crystals, where the cut-off phonon energy $h\omega_{max}$ is usually higher than 1000 cm^{-1} only the first one is involved in luminescence phenomena. Results of Judd–Ofelt analysis of fluorescence characteristics of materials investigated are gathered in Table 7. It can be seen that among possible transitions between the $^4F(3)_{9/2}$ metastable multiplet and multiplets belonging to terms ^6H and ^6F the transition between $^4F(3)_{9/2}$ and $^6H_{13/2}$ multiplets is characterized by the highest rate value. This observation is

consistent with polarized room temperature emission spectra of both the crystals.

It follows from the Judd–Ofelt analysis that more than 90% photons are emitted in four transitions ending on $^6H_{15/2}$, $^6H_{13/2}$, $^6H_{11/2}$, and $^6H_{9/2}$ multiplets. Taking this into account experimental branching ratios were calculated by numerical integration of unpolarized emission spectra recording exploiting low resolution monochromator coupled with Si CCD camera, that exhibits linear response in 350–1000 nm range. Results of calculation are shown in last column of Table 7.

Emission spectra recorded at liquid helium temperature are shown in Fig. 7a and b. In contrast to high anisotropy of absorption spectra, emission spectra do not show significant polarization dependence. With ascending temperature small shift of υ_{max} to lower energies and increase of FWHM of lines appear.

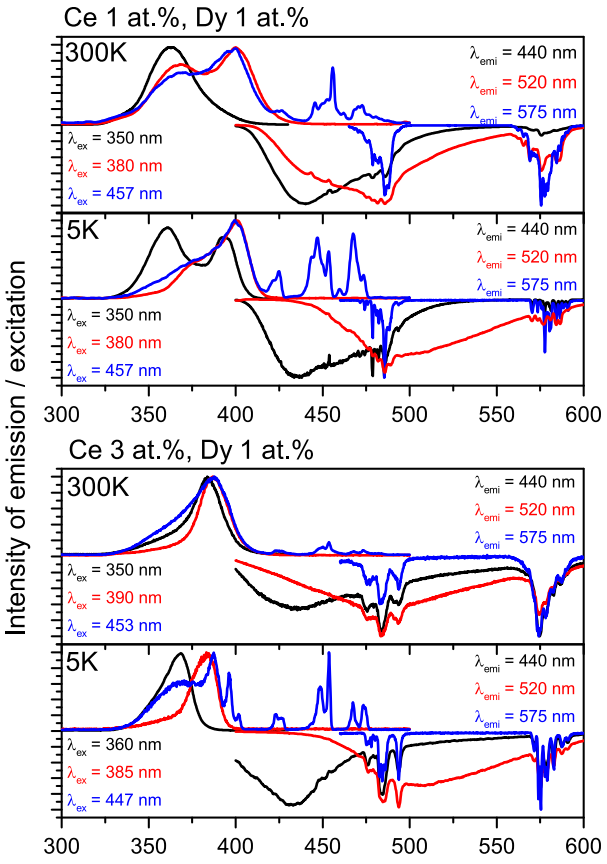

Fig. 6. Emission and excitation spectra, recorded for different: (1) excitation and (2) observation wavelengths, (3) concentration of cerium and (4) temperature. Strong influence of optical anisotropy is clearly seen. All spectra were normalized to their maxima. (For interpretation of the references to color in this figure legend, the reader is referred to the web version of this article.)

7. Excited state relaxation kinetics

In investigated materials two luminescent ions are embedded. Luminescence form Ce^{3+} ions, related to allowed 5d–4f transitions, is characterized by broad and fast-decaying bands. Contrary to Ce^{3+}, emission from Dy^{3+} ions, related to forbidden 4f–4f transitions, appears as narrow lines which decay in microsecond timescale. Cerium was incorporated in order to sensibilize dysprosium ions luminescence. We were motivated by the idea of energy transfer from cerium ions, which are easily to excite due to strong and broad absorption bands, to dysprosium ions, which are tough to excite due to lack of strong absorption lines. An experimental evidence of energy transfer is shortage of lifetime of "donor" in the presence of "acceptor" contrary to donor's lifetime in sample devoid of acceptors. To investigate if energy transfer phenomenon occurs, luminescence decay measurements in function of temperature and excitation wavelength were performed.

When concerning lifetime of luminescent centers responsible for broad emission lines in 400–600 nm region, their value decreased from 60 ns in 5 K to 40 ns in 300 K, for sample doped with 3 at% of Ce, and from 40 ns in 5 K to 20 ns in 300 K for second sample. Shortage of lifetime with ascending temperature is an evidence of rising of energy transfer rate between Ce and Dy ions.

In order to measure lifetime of $^4F_{9/2}$ metastable level, samples were excited by 475 nm, into band related to $^6H_{15/2}$–$^4F_{9/2}$ transition, when luminescence was monitored at 585 nm (transition to first excited state). Temperature, in the range 5–300 K, does not affect lifetime of metastable level in a significant way. For sample

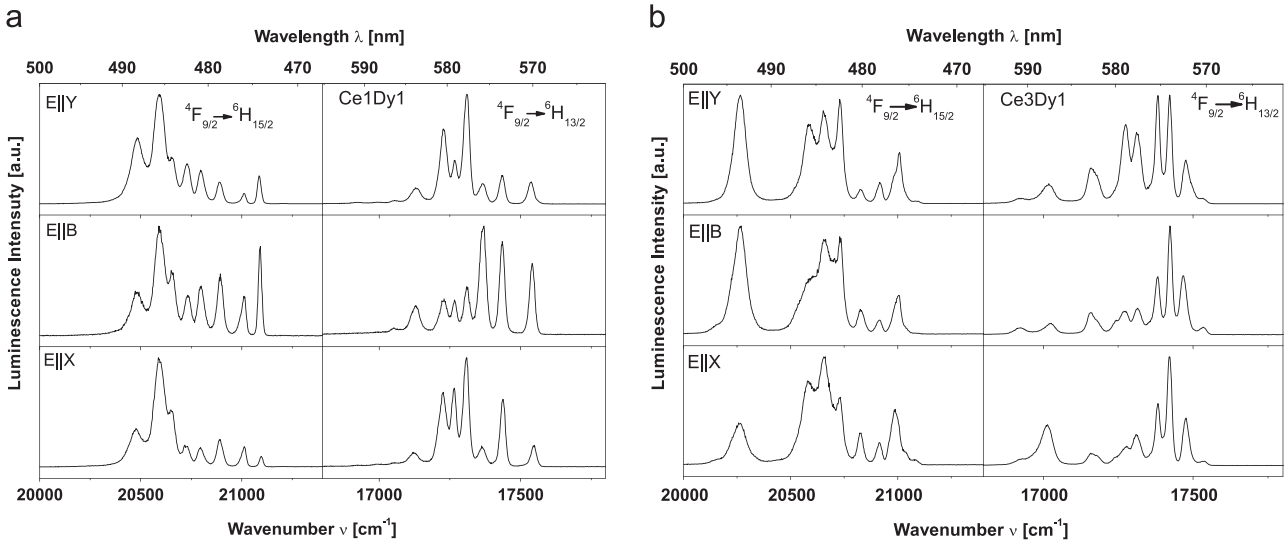

Fig. 7. (a) High resolution polarized, low temperature (5 K), emission spectra of investigated sample doped with 1 at% of Ce. Influence of optical anisotropy on shape of band and intensity of lines is high. All spectra were normalized to their maxima, thus their intensities should not be compared. (b) High resolution polarized, low temperature (5 K), emission spectra of investigated sample doped with 3 at% of Ce. Influence of optical anisotropy on shape of band and intensity of lines is high. All spectra were normalized to their maxima, thus their intensities should not be compared.

doped with 1 at% of cerium value of t_{exp} oscillates around 0.45 ms, while for sample doped with 3 at% of cerium varies around 0.5 ms. For both the samples in all temperature ranges decay curves exhibit single exponential shape. With regard to the obtained values of radiative lifetimes from Judd–Ofelt analysis (0.45 ms; 0.43 ms), quantum efficiencies of concerned level are high. Obtained values of τ_{rad} are ca. 10% smaller contrary to τ_{exp}. This situation emerges most probably from two reasons: (1) exact concentration of Dy in both the samples is unknown, for calculations we used nominal concentration of 1 at% and (2) we did not perform full crystal field calculations for investigated materials, thus we were obligated to use $\|U^t\|$ parameters that are correct for borosulphate glass [15]. The mismatch of values of doubly reduced parameters between borosulphate glass and LGSO should be small, but can slightly affect obtained Ω_t and τ_{rad} parameters.

8. Optical amplification measurements

Due to the reported potential of Dy^{3+} doped glasses and crystals as optical gain medium for the emission associated with the transition $^4F_{9/2} \rightarrow {}^6H_{13/2}$ (575 nm) [6] this capability has been researched for the reported samples. But in our experiments the Dy^{3+} ions have been excited through transfer processes from the Ce^{3+} ions.

In general, when a probe beam passes through a solid medium, its intensity decreases from the initial I_0 value to the final $I_{probe}(L)$ value according to the known Lambert–Beer law

$$I_{probe}(L) = I_0 e^{-\alpha L} \tag{2}$$

where α and L are the absorption coefficient and the length of the sample, respectively (L=0.2 mm). When the pump and the probe are simultaneously switched on, the intensity recorded from the sample luminescence at the probe wavelength, I_{pp}, will be given by

$$I_{pp} = I_p + I_0 e^{(g_{int}-\alpha)L} \tag{3}$$

where I_p is the spontaneous emission intensity induced by the pumping radiation and g_{int} is the internal gain coefficient. Then, the optical gain coefficient g can be expressed as

$$g = g_{int} - \alpha \tag{4}$$

The signal enhancement (SE) is defined as

$$SE = \frac{I_{pp} - I_p}{I_{probe}} \tag{5}$$

By introducing Eqs. (3) and (4) in expression (5), SE can be related directly with the optical gain coefficient as follows:

$$SE = e^{g_{int}L} \tag{6}$$

The intensities I_p, I_{pp} and I_{probe} can be experimentally measured. As we use a pulsed excitation source, I_p and I_{pp} are experimental curves that decay after the excitation pulse. As a result of applying Eq. (5) to these experimental curves the temporal evolution of the signal enhancement is obtained, as can be seen in Fig. 8. For these measurements the laser excitation was carried out at 359 nm in the absorption of Ce^{3+} ions and the detection of the 575 nm emission of Dy under laser excitation at 359 nm with a density power of 5.6 mJ/cm^2 and the probe syntonized at 575 nm. A rapid increase immediately after the laser pulse excitation can be appreciated for both the samples, reaching values greater than 1 which proves the enhancement of the signal. Different maxima values are reached by both the samples, the highest being obtained in the sample codoped with Dy 1 at% and Ce 1 at%, with an SE value of 1.74. For this sample, the maximum SE and the gain

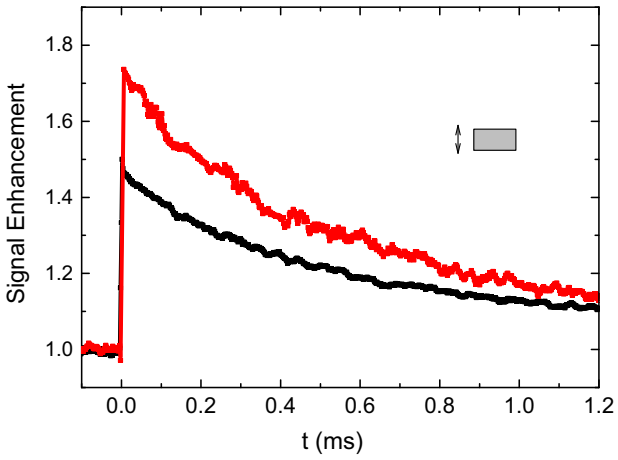

Fig. 8. Temporal evolution of the signal enhancement at 575 nm for the samples doped with Dy 1 at% and Ce 1 at% (red curve) and Dy 1 at% and Ce 3 at% (black curve) under laser excitation at 359 nm with a density power of 5.6 mJ/cm^2. (For interpretation of the references to color in this figure legend, the reader is referred to the web version of this article.)

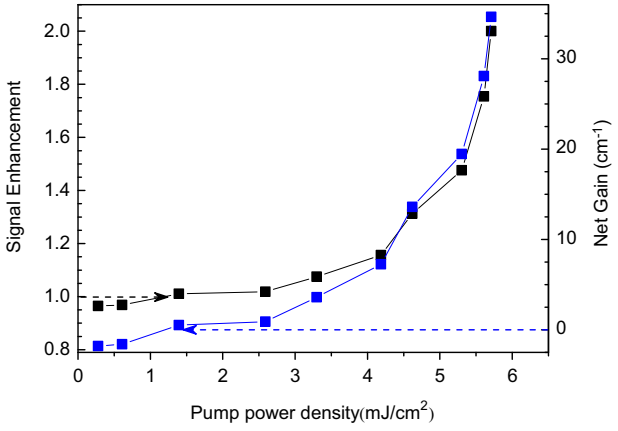

Fig. 9. Signal enhancement and gain at 575 nm of the sample doped with Dy 1 at% and Ce 1 at% as a function of the pump power density. The arrows show the thresholds from which the magnitudes reflect increase of the signal enhancement and positive gain.

coefficient as functions of the pump energy density are given in Fig. 9. A continuous growth of both magnitudes with the pump power density can be noticed; the arrows in Fig. 9 point to the threshold at 1.40 mJ/cm^2 from which there is a signal enhancement (>1) and the optical gain turns positive. The maximum value for the gain has been observed for a pump energy density of 5.7 mJ/cm^2 corresponding to 34 cm^{-1} during the maximum detected intensity. Comparing this result with the gain of 1.9 cm^{-1} for a Dy:$LiNbO_3$ crystal reported in Ref. [6] there is a clear improvement accomplished with the $(Lu_{0.2}Gd_{0.78}Ce_{0.01}Dy_{0.01})_2SiO_5$. Such high value for the gain is suspected to be supported by the strong absorption of the laser excitation at 359 nm by Ce ions and the efficient transfer to the Dy ions accomplished in the reported crystals.

9. Conclusions

Motivation to incorporate cerium ions was to enhance dysprosium luminescence due to energy transfer from excited cerium ions. It has been found that cerium incorporation can force phase transition in LGSO crystals with Lu/Gd ratio close to eutectic point. Both crystals exhibit strong optical anisotropy in absorption and

emission spectra. Investigated materials possess wealth luminescent properties due to three factors as follows: optical anisotropy, at least three luminescent centers and moderate energy transfer between those centers. According to these facts description of optical properties of investigated materials was a tough task, because luminescence properties change depending on excitation, polarization and temperature. Conducted crystallographic considerations lead to conclusion, that in GSO structure, occurrence of Ce^{4+} cations is quite possible. In vicinity of these ions creation of point defects is highly possible due to charge mismatch.

Calculations in framework of Judd–Ofelt model were carried out, and obtained results were compared with experimental ones. Evaluated JO parameters were used to calculate lifetime of metastable level and luminescence branching ratios. Experimental β are in good confirmation to the calculated one, which additionally confirms proper evaluation.

Optical amplification in these samples was evaluated by means of a pump and probe experiment, with a positive result. A high gain coefficient of 34 cm^{-1} at the 575 nm emission under 359 nm excitation with a density power of 5.7 mJ/cm^2 was found in the sample codoped with Dy 1 at% and Ce 1 at%. This high value supports the potential of the $(Lu_{0.2}Gd_{0.78}Ce_{0.01}Dy_{0.01})_2SiO_5$ as an efficient gain medium.

Acknowledgment

The work received financial support from National Center of Science of Poland under Grant agreement no. DEC2011/03/B/ST2/02622.

I. R. Martin and C. Pérez-Rodríguez wish to thank Ministerio de Economía y Competitividad of Spain (MINECO) within the National Program of Materials (MAT2010-21270-C04-02/-03/-04) and the Fundamental Research Program (FIS2012-38244-C02-01), the > Consolider-Ingenio 2010 Program (MALTA CSD2007-0045, www.malta-consolider.com), the EU-FEDER for their financial support, the FSE and ACIISI of Gobierno de Canarias for the Project ID20100152 and FPI Grant.

References

[1] B. Liu, M. Gu, Z. Qi, C. Shi, M. Yin, G. Ren, J. Lumin. 127 (2007) 645.
[2] G. Dominak–Dzik, W. Ryba-Romanowski, R. Liseicki, P. Solarz, M. Berkowski, Appl. Phys. B 99 (2010) 285.
[3] M. Jacquemet, C. Jacquemet, N. Janle, F. Druon, F. Balembois, P. Georges, J. Petit, B. Viana, D. Viven, B. Ferrand, J. Appl. Phys. B 80 (2005) 171.
[4] M. Glowacki, et al., J. Solid State Chem. 186 (2012) 268.
[5] O. Sidletskiy, V. Bondar, B. Grinyov, D. Kurtsev, V. Baumer, K. Belikov, K. Katrunov, N. Starzhinsky, O. Tarasenko, V. Tarasov, O. Zelenskaya, J. Cryst. Growth 312 (2010) 601.
[6] P. Haro-Gonzalez, et al., Opt. Mater. 33 (2010) 196.
[7] G. Dominiak-Dzik, et al., Cryst. Growth Des. 10 (2010) 3521.
[7a] R. Lisiecki, G. Dominiak-Dzik, P. Solarz, W. Ryba-Romanowski, M. Berkowski, M. Głowacki, Appl. Phys. B 98 (2010) 337–346.
[8] C.K. Jayasankar, E. Rukmini, Physica B240 (1997) 273.
[9] (a) J. Xu, et al., J. Cryst. Growth 277 (2005) 175;
(b) J. Xu, et al., J. Cryst. Growth 281 (2005) 411.
[10] G.H. Dieke, Spectra and Energy Levels of Rare Earth Ions in Crystals, Interscience Publishers, New York, 1968.
[11] B.R. Judd, Phys. Rev. 127 (1962) 750.
[12] G.S. Ofelt, J. Chem. Phys. 37 (1962) 511.
[13] A.J. Wójtowicz, K. Wiśniewski, M. Ptaszyk, VUV Studies of Energy Transfer Processes in GSO:Ce (Hasylab Annual Report), 2004.
[14] W. Drozdowski, A.J. Wójtowicz, D. Wiśniewski, P. Szupryczyński, Studies of Two Cerium Sites in Lu_2SiO_5:Ce and Y_2SiO_5:Ce (Hasylab Annual Report), 2002.
[15] R. Praveena, R. Vijaya, C.K. Jayasankar, Spectrochim. Acta A 70 (2008) 577.
[16] T. Gustafsson, M. Klintenberg, S.E. Derenzo, M.J. Weber, J.O. Thomas, Acta Crystallogr. C 57 (2001) 668.
[17] Yu.I. Smolin, S.P. Tkachev, Sov. Phys. Crystallogr. 14 (1969) 14.